

Removing wave effects from the wind stress vector

Karl F. Rieder and Jerome A. Smith

Marine Physical Laboratory, Scripps Institution of Oceanography, La Jolla, California

Abstract. The presence of ocean surface waves has been observed to affect both the magnitude and direction of the wind stress. Here concurrent wind and wave data are employed to study their relationship. To help isolate the influence of the waves, the wind stress is broken into three frequency bands: “low” (frequencies below 0.06 Hz), corresponding to large-scale motions in the boundary layer at frequencies below any significant wave energy; “middle” (frequencies between 0.06 and 0.16 Hz), corresponding to the frequencies of the dominant swell and wind waves; and “high” (frequencies above 0.16 Hz), corresponding to waves too short to influence coherently the wind fluctuations at the anemometer site 8 m above the surface. Most often, the low band holds the most stress. The magnitude of the wind stress within the low band increases roughly with the square of the mean wind speed, the high band appears to increase with the wind speed to the fourth power, and the middle band exhibits varied dependence. The direction of the wind stress in the low band is closely tied to the mean wind direction. In contrast, the directions in the middle and high bands are influenced by the waves and can be significantly off the mean wind direction. The middle band is biased toward the direction of long-period swell, while the high band is biased toward the direction of short-period seas, which is closer to the wind direction. Thus it is mainly within the middle band that large deviations in stress versus wind magnitude and direction are found. To further isolate the influence of waves, a wave-correlated fraction of the wind stress is estimated using direct correlations between the surface elevation and wind fluctuations. Removing this wave-correlated stress from the total results in a residual stress that is better behaved: the magnitude of the residual stress in the middle band is modeled by a simple wind speed dependent drag coefficient, and the direction is very nearly aligned with the wind in both the middle and high bands. These results indicate that waves are indeed closely associated with the observed deviations from “bulk formula” stress estimates. They also suggest a new method by which to estimate the wind stress; namely, partitioning the stress into three separately modeled parts: a low-frequency stress, a high-frequency wave-correlated stress, and a high-frequency residual stress.

1. Introduction

Wind stress is perhaps the most dynamically significant exchange across the air-sea interface. It has long been recognized that wind stress is fairly well related to the square of the wind speed and that some improvement of this relation is obtained by including stability effects [Businger *et al.*, 1971]. This is usually parameterized via the bulk formula

$$\tau = \rho C_d |\mathbf{U}| \mathbf{U}, \quad (1)$$

where τ is the stress, ρ is the air density, \mathbf{U} is the windspeed, and C_d is the drag coefficient, which can be regarded as a function of stability. Over water, it is also recognized that there remains considerable additional variability in the relation between stress and wind, in which surface waves play an important part. Most previous work has concentrated on adjusting the magnitude of the stress (via the drag coefficient) according to some function of “wave age,” defined as the ratio of wave phase velocity over wind speed

[e.g., Donelan 1982]. However, both the magnitudes and directions have been observed to deviate significantly from bulk estimates in the presence of swell [Dobson *et al.*, 1993, Geernaert *et al.*, 1993, Rieder *et al.*, 1994]. In at least one case, a systematic directional deviation of up to 30° persists for most of the 10 days examined [Rieder, *et al.*, 1994]. Clearly, no scalar adjustment can cause the directions to come to agreement for such cases. Thus wave age scaling alone can apparently help only in the absence of swell [Donelan *et al.*, 1993]. Unfortunately, this condition represents only a small fraction of the global oceans.

Here we investigate the extent to which such “stress deviations” can be accounted for by motions that are directly correlated with fluctuations of the sea surface. The data employed were gathered during the Marine Boundary Layer Experiment (MBLEX) leg 1 (February - March 1995) using a sonic anemometer and a set of wave wires deployed off the Floating Instrumentation Platform (FLIP). We employ two techniques to help isolate the influence of the waves.

First, we make use of the fact that the significant wave energy occurs over a smaller frequency band than the wind stress. The wind stress can be calculated as a function of frequency via the cospectra C_o between the downwind u' , crosswind v' and vertical w' fluctuating velocities:

Copyright 1998 by the American Geophysical Union.

Paper number 97JC02571.
0148-0227/98/97JC-02571 \$09.00

$$\tau = Co_{u'w'}(f)\mathbf{i} + Co_{v'w'}(f)\mathbf{j}, \quad (2)$$

where f is the frequency, \mathbf{i} is the unit vector in the u' direction, and \mathbf{j} is the unit vector in the v' direction. The total stress is the integral over all frequencies of τ . In practice, the wind stress comes from turbulent wind fluctuations at frequencies principally between 0.002 and 1 Hz (periods of 500 and 1 s, respectively), while the dominant wave energy is at frequencies between 0.05 and 0.5 Hz (periods of 20 and 2 s, respectively). By examining the stress in a limited band, we can focus more clearly on the wave influence. Thus the wind stress is first broken into three bands of similar magnitude: the low-, middle-, and high-frequency bands. The low-frequency band cannot have much direct correlation with the surface elevation, since negligible wave energy occurs there. The high-frequency band is tied to the shortest waves, which respond quickly to changes in wind speed and direction and hence are roughly in dynamic equilibrium with the wind. In the middle band, the waves are large and rarely in equilibrium with the wind and are often mis-aligned. Thus it is mainly in the middle band that the waves can change the stress significantly.

Second, we estimate complex cross-spectra between the fluctuations in the wind and the sea surface elevation (including both amplitude and phase). This applies primarily to the middle band of stress frequencies, since there are negligible waves in the low band and the waves corresponding to the high band do not produce much correlation at a height of 8 m above the surface. We then

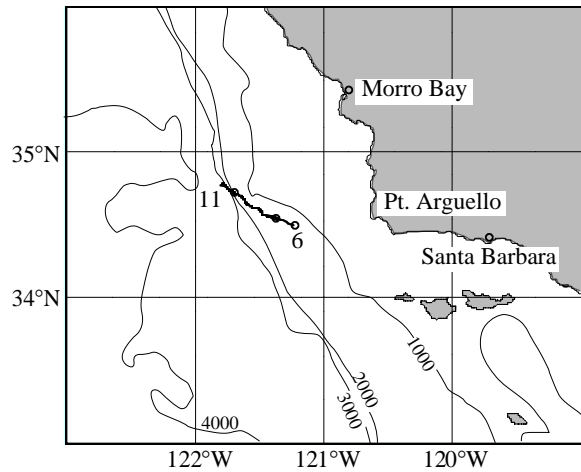


Figure 1. Site of the Marine Boundary Layer Experiment (MBLEX) leg 1. The Floating Instrumentation Platform (FLIP) was located due west of Point Arguello when the mooring line was cut on March 7. FLIP then freely drifted NW during the remainder of the cruise, March 7-11, 1995.

estimate the (vector) stress accounted for by these correlated air fluctuations and subtract it. The essential question is whether removing this surface-correlated fraction also removes the anomalous magnitudes and directions from the estimated stress. If so (as we find), the implication is that it is indeed the waves that cause these anomalies. In addition, this suggests a new approach by which to isolate this wave influence for further study.

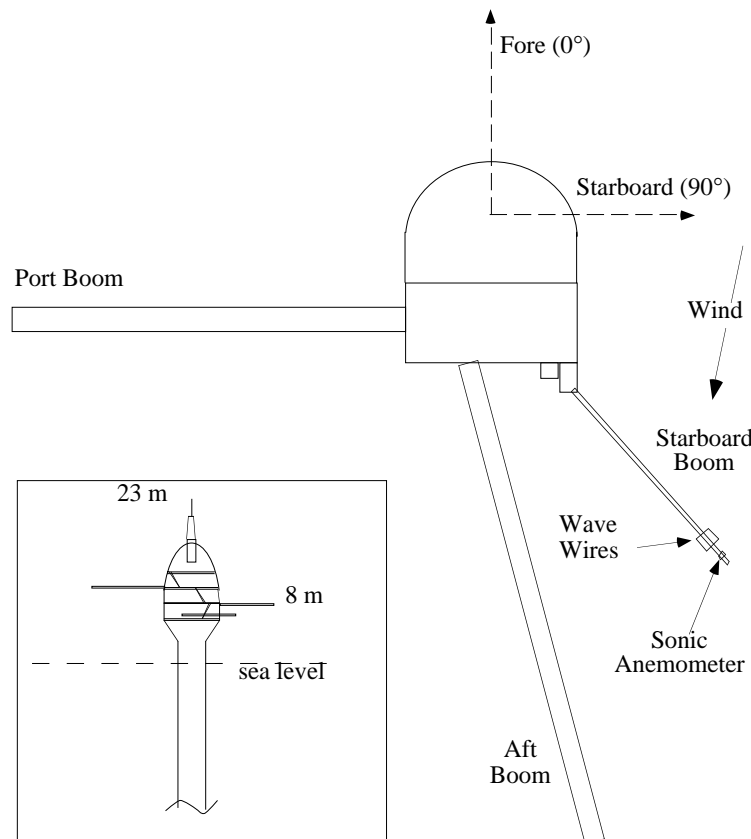


Figure 2. Plan view of FLIP. Principal instruments for this study, one sonic anemometer and a four wire wave array, were deployed together from the starboard boom at 8 m above mean sea level. This placed the anemometer in clear air while FLIP was adrift.

2. Marine Boundary Layer Experiment

The Marine Boundary Layer Experiment consisted of two 1-month-long legs in the winter and spring of 1995. The data for this study were collected during MBL leg 1 from March 4 to 12. The instruments were deployed from FLIP at an open ocean site approximately 30 miles off Point Arguello, California. The weather during the study period was dominated by the passing of a low-pressure trough. On March 7, the wind slowed from 10 to 3 m/s as the front passed. The wind turned nearly 180° early on March 8 and increased to almost 15 m/s over the course of the day. The next 2 days brought sustained winds near 15 m/s, with nearly constant wind direction, finally culminating in a series of squall lines accompanied by heavy rain on March 10. FLIP was deployed with a one-point mooring at the start of leg 1, but as winds increased, FLIP was pushed by a strong current opposing the wind, and the mooring line had to be cut on March 6 to avoid tangling. From then on, FLIP drifted freely, following a track to the northwest (Figure 1).

During MBL leg 1, a sonic anemometer and a wave array of four resistance wires were collocated on the starboard boom, 8 m above mean sea level (see Figure 2 inset). When freely drifting, FLIP turns in response to the wind, placing the sonic anemometer in clear air off to the side of the superstructure (Figure 2). Complementary

measurements of the mean wind speed and direction, air temperature, and humidity were made atop FLIP's mast at 23 m above mean sea level. Sea surface temperature was measured by a surface-following float loosely tethered from the lowest deck.

The wave wires measured sea surface elevation on the corners of a square 1 m on the diagonal. The data were filtered to 1.33 Hz and corrected for FLIP motion using estimates of FLIP's tilt (from a three-component magnetic flux measurement) and acceleration (from a three-component accelerometer set). Wave directional spectra were calculated from these elevation measurements using a simple "tilt-and-roll" formulation first suggested by *Longuet-Higgins et al.* [1963] and reviewed by *O'Reilly et al.* [1996]. This provides good estimates of wave energy and directionality between frequencies of 0.085 and 0.6 Hz (periods of 12 and 1.5 s, respectively). This was verified by comparison of the empirical wavenumber with that from linear dispersion for surface gravity waves. The empirical wavenumber is estimated as the square root of the ratio of the sea surface slope spectrum to the elevation spectrum. Theoretical and empirical wavenumbers match well above 0.10 Hz but diverge below 0.085 Hz (12-s period). The excellent fit at frequencies above 0.10 Hz corroborates the accuracy of the wave wire system, indicating its ability to resolve waves with lengths from 1 to 200 m.

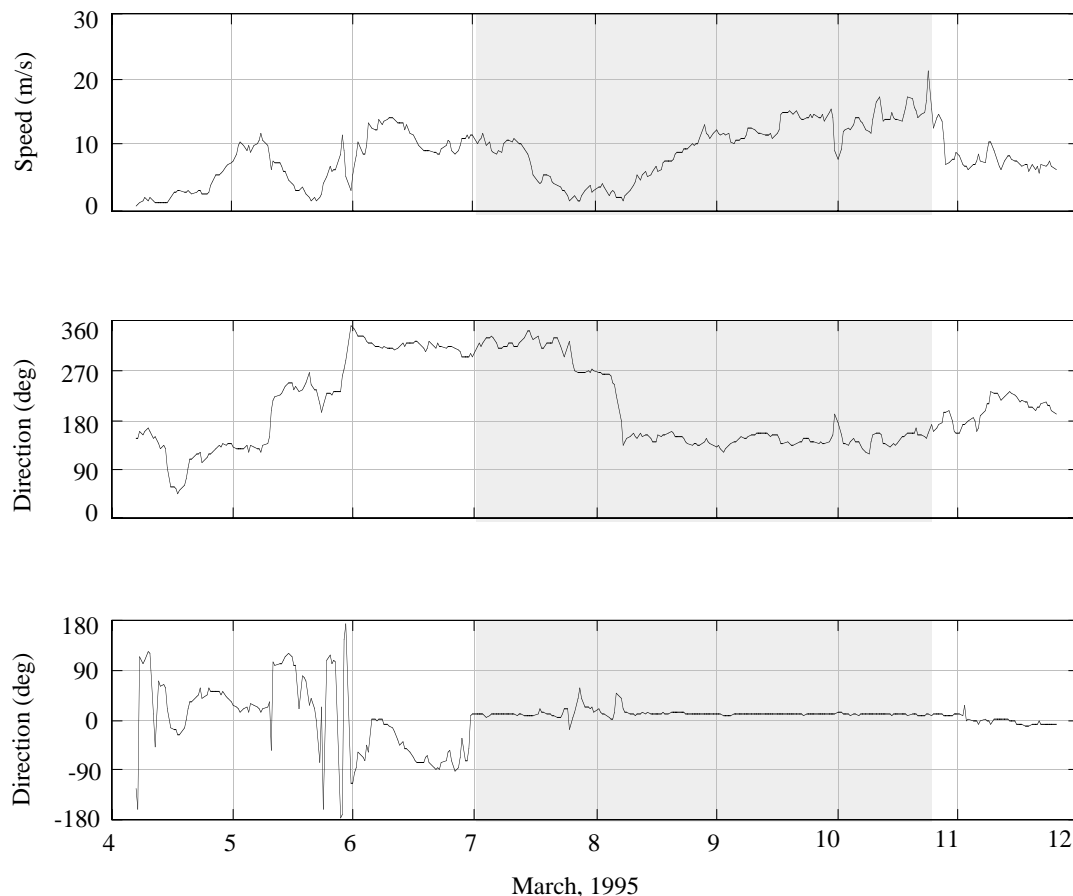


Figure 3. (top) Wind speed, (middle) direction, and (bottom) direction relative to FLIP over the course of MBL leg 1. The shaded region indicates the period used in this study, beginning just after the cut of the mooring line and ending just prior to the fall of the wind marking the end of the strong wind event. This event saw a dramatic turning and increase of the wind, with high speeds and steady direction prevailing for 2 days. While FLIP was freely drifting, the wind direction was favorable, putting the sonic anemometer in clear air, as indicated by the positive relative wind direction.

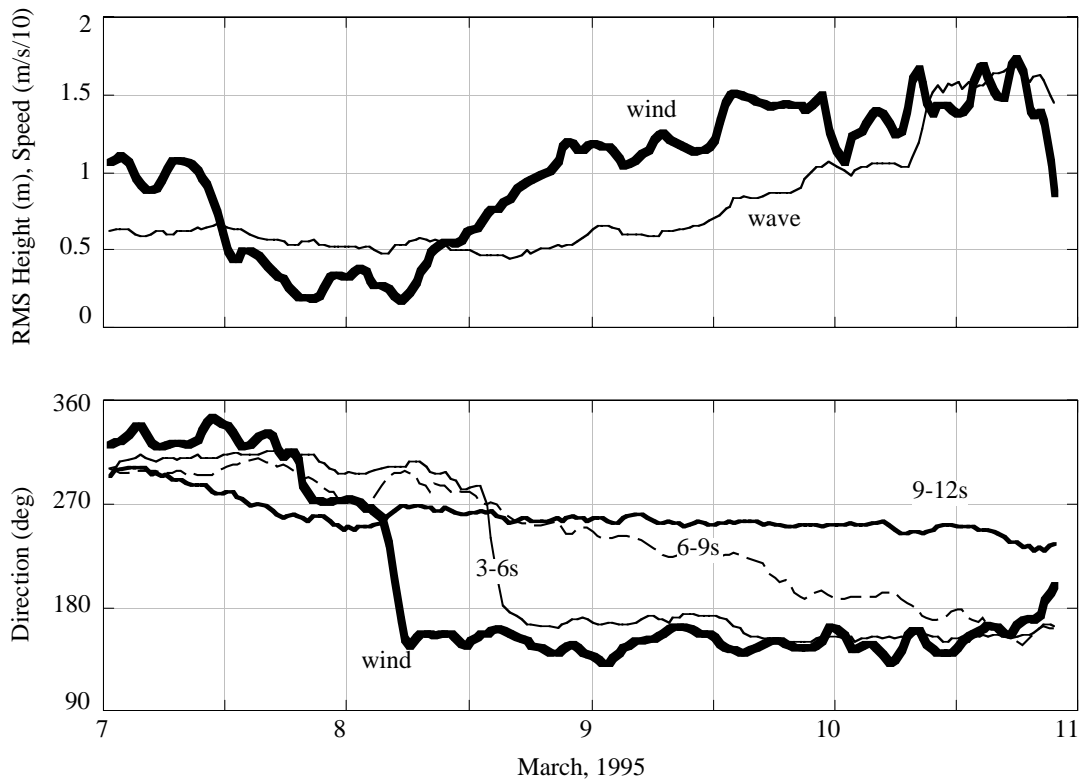


Figure 4. (top) Wind speed and wave height and (bottom) wind and wave directions during the study period. The highest-frequency waves (3-6 s) respond most quickly to the turning and increase of the wind, while the lowest-frequency swell waves (9-12 s) are affected little by the changing wind.

The sonic anemometer provides estimates of the three components of the wind velocity at 5 Hz. From these, the wind stress is directly estimated via the eddy correlation method. Reliable measurements of the wind stress are difficult to make at sea, and several important issues need to be addressed.

1. The anemometer may be sheltered by the hull. Irregular stress measurements result when the sonic anemometer is even partially in the lee of FLIP [Rieder *et al.* 1994]. While moored, the direction of the wind relative to FLIP varies, with the anemometer going in and out of FLIP's wake. While freely drifting, FLIP rotates in response to the wind, placing the sonic anemometer in clear air. Following the cutting of the mooring line, the relative wind direction stays slightly above 0° , indicating wind directed from slightly starboard of forward (Figure 3). The mean declination of the wind vector can also indicate shadowing. Large declinations are measured during periods when the sonic anemometer is in FLIP's lee, but during free drift, the mean declination remains near zero. A subsection of the available data is selected for this study: from early on March 7, beginning just after the cutting of the mooring, to late March 10, ending just prior to the fall of the wind speed at the end of the strong wind event. This period is indicated by shading in Figure 3.
2. To help improve the statistical reliability of stress estimates, wind speeds are sometimes required to be greater than 3 or 4 m/s. This criterion is not enforced here, as such cases are few and continuity of the time series is of interest. The low wind speed periods ($U < 4$ m/s) can have relatively large drag coefficients (>0.002), as will be discussed later.

3. Atmospheric stability affects both the magnitude and direction of the wind stress and is most important at low wind speeds [Businger *et al.*, 1971, Geernaert, 1988]. The stability parameter, z/L (z is the measurement height and L is the Monin-Obukhov length), is calculated using the fast-sampled wind velocity and air temperature from the sonic anemometer data, humidity from the dew point hygrometer, and sea temperature from the surface float [cf. Large and Pond, 1981]. Periods with wind speeds greater than 5 m/s are characterized by near-neutral stability ($0 > z/L > -0.5$); for wind speeds greater than 10 m/s, conditions were neutral ($|z/L| < 0.05$). The remaining low wind speed periods (March 7) were either neutral or slightly unstable. However, since it is unclear how to correct for stability when considering only a particular frequency band of the wind stress, no corrections are made on the data. The important point, though, is that stability effects cannot explain the modifications of the wind stress that are seen at all wind speeds.
4. Motion of the anemometer can contaminate the measurements. FLIP's motion was studied in detail by [Smith and Rieder, 1997], using data from the Surface Wave Processes Program (SWAPP), in which FLIP was in a three-point moor. The results indicate that the motion at the instrument location is generally small: the fluctuating tilts are of order 1° rms (mostly near the resonant tilt period of 56 s), and induced velocities are a few centimeters per second, at most. The estimated effect on the measured total wind stress was negligible (order 3% or less) for the high-wind cases previously analyzed from the SWAPP data set. In free drift, the motion is generally smaller. In this study, we investigate fractional

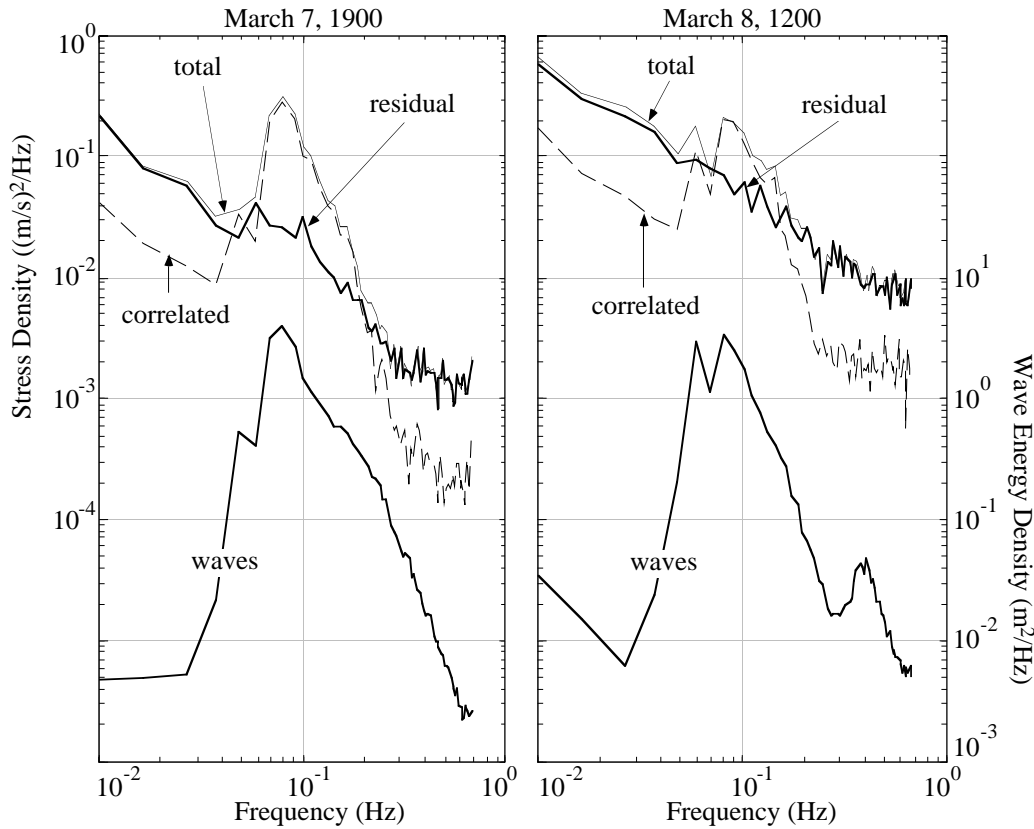


Figure 5. Wave-correlated, residual, and total stress spectra versus frequency for the period around (left) March 7, 19:00 and (right) March 8, 12:00. A wave influence is represented by the strong peak in each spectra at the dominant wave frequencies. In the middle band (0.06-0.16 Hz), the wave-correlated stress is a large fraction of the total, especially for the first, low wind-speed period.

portions of the stress from specific frequency bands; any motion contamination will become increasingly more important, particularly in the middle “wave” band where the largest motion-induced velocities occur. Using the tilt and acceleration measurements of the superstructure, the anemometer is leveled and the motion-induced vertical and horizontal velocities subtracted at each 0.75 s time step. The effect of these motion corrections is discussed further in section 3.

Wind speed, rms wave height, and wind and wave directions during the study period are shown in Figure 4, smoothed with a 90-min running mean filter. The high-frequency “equilibrium range” waves (3 to 6 s) respond quickly to the turning of the wind. The 6 to 9 s waves remain misaligned for a while but steadily grow in the downwind direction and eventually become aligned with the wind. The low-frequency swell, in contrast, is affected little by the turning and increasing of the wind, maintaining a near-constant direction throughout the study period. After the turning, the swell propagates at nearly a right angle to the wind.

3. Approach

We seek the direct influence of waves on wind stress. To this end, we start with the co-spectral description of the stress, as outlined in (2), and divide this into three frequency bands: (1) low, below significant surface wave energy, defined as below 0.06 Hz for the data considered here; (2)

middle or “wave band,” where correlations with surface elevations can be expected to show up at the 8-m anemometer height, taken here to be a 0.06- to 0.16-Hz band; and (3) high, corresponding to wavelengths too short to maintain direct correlation up to 8 m above the surface. As a guide, we take this to be the frequency corresponding to $k=1/8$ m, or about 0.16 Hz (wave-induced fluctuations in the wind field are theorized to decay with height by the inverse of the wavenumber).

To further isolate the direct wave influence, we next break the middle- and high-frequency bands into a “correlated” and “residual” stress. We define the correlated stress estimate using complex cross-spectra C between horizontal u' , v' and vertical w' fluctuating air velocities and the sea surface elevation ζ at 1.33 Hz:

$$\tau_{\text{corr}}(f) \equiv \frac{\text{Re}[C_{u'\zeta}(f)C_{w'\zeta}^*]}{C_{\zeta\zeta}} \mathbf{i} + \frac{\text{Re}[C_{v'\zeta}(f)C_{w'\zeta}^*]}{C_{\zeta\zeta}} \mathbf{j}, \quad (3)$$

where asterisks denote complex conjugation, and \mathbf{i} and \mathbf{j} are unit vectors in the x and y directions. This expression includes both inphase and quadrature motions in the resulting estimates of wave-correlated wind stress. The “residual stress” is calculated as the vector difference between the total stress and this correlated stress estimate.

The wave-induced motions in the air just above the surface should result in a stress roughly equivalent to the direct input of momentum from the wind to the waves

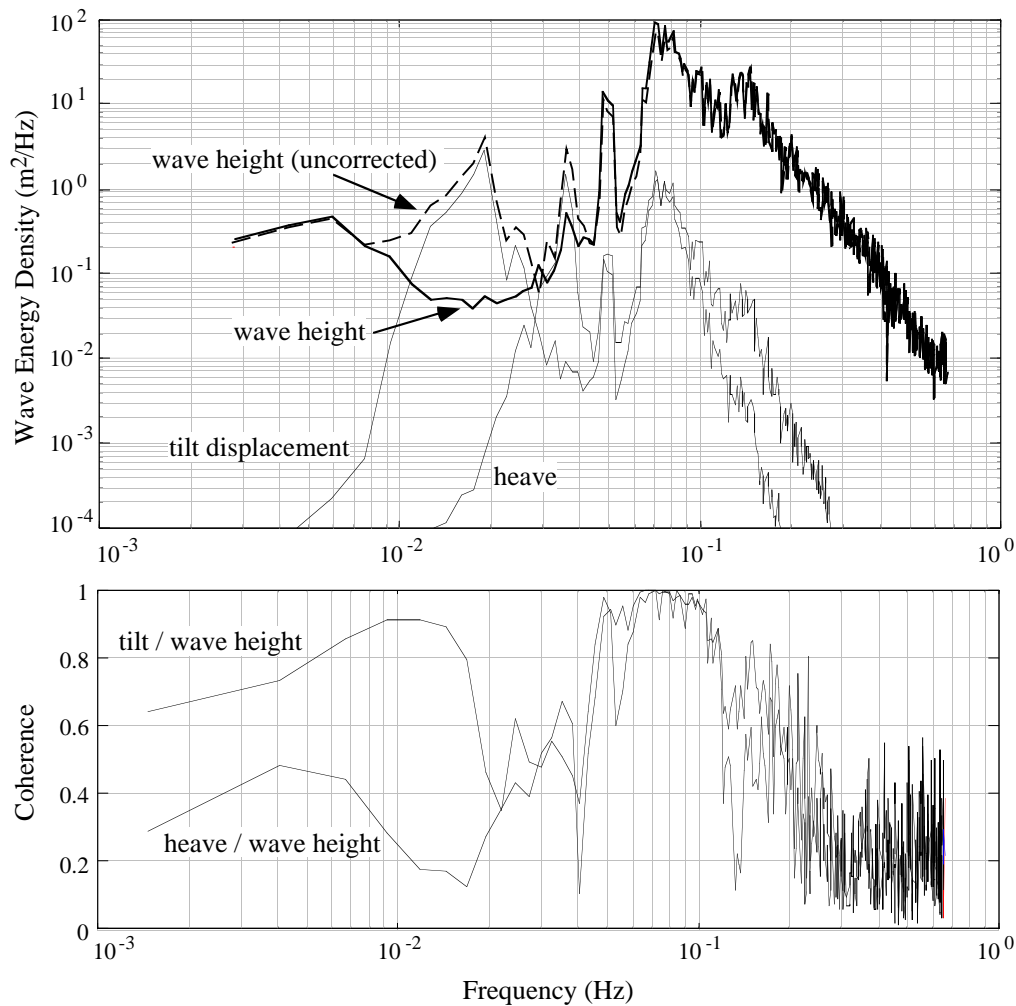


Figure 6. Power spectra for the motion-corrected and motion-uncorrected surface elevation, tilt-induced displacement at the instrument location, and heave. Surface displacements are more than an order of magnitude larger than FLIP motions at the principal wave frequencies but are significantly smaller at the resonant frequencies of motion (tilt, 0.017 or 58 s period; heave, 0.038 Hz or 26 s period). Correction of the elevation results in a 70% reduction at the resonant frequencies of FLIP and less than a 4% modification at wave frequencies.

[Janssen, 1989]. With wind fluctuations measured at a finite height above the surface, this is expected to yield an underestimate for correlations with higher-frequency waves. At low frequencies, where little wave energy exists, true correlations between waves and wind should be small. However, owing to the large wind stress at these frequencies and to direct forcing of FLIP by the low frequency wind fluctuations, any small error in the motion correction (especially near the resonant frequencies) can yield spurious large values for the “wave-correlated” stress. We therefore do not attempt this calculation for the low-frequency band. The variability of the wind stress in the low-frequency band is left to other studies.

The wave-correlated, residual, and total stress spectra are plotted against frequency in Figure 5 for data from two 3-hour segments near March 7, 1900 UTC and March 8, 1200 UTC. The cross spectra are computed from 6 consecutive half-hour time segments and band averaged over 16 frequencies, yielding about 96 degrees of freedom. The wave influence is represented by a strong peak in the wave-correlated and total stress spectra at the dominant wave

frequencies. For the first time segment, when wind speeds were low, the wave-correlated stress represents nearly all the stress in the middle band (between frequencies of 0.06 and 0.16 Hz or periods of 16 and 6 s, respectively). Outside these limits, the power in the correlated stress spectrum is nearly an order of magnitude below the total. During the second segment, the wind was stronger and the stress over all frequencies rises, making the peak at the wave frequencies less visible. In contrast, the residual stress maintains a form that is both simpler and more consistent between the two cases.

FLIP motions are modest, but should be considered. During a sample 3 hour period when conditions remained nearly constant (March 10, 9:00-12:00) and wind speeds and wave heights were large ($U_8 = 14.1$ m/s and $H_{rms} = 1.48$ m), the rms tilt in the direction of the starboard boom was only 0.66° (corresponding to 0.22 m of displacement at the anemometer) and rms heave was only 0.16 m. The spectra of the motion-corrected and motion-uncorrected wave height, the tilt-induced vertical displacement, and heave are plotted in Figure 6. Heave and tilt displacements are more

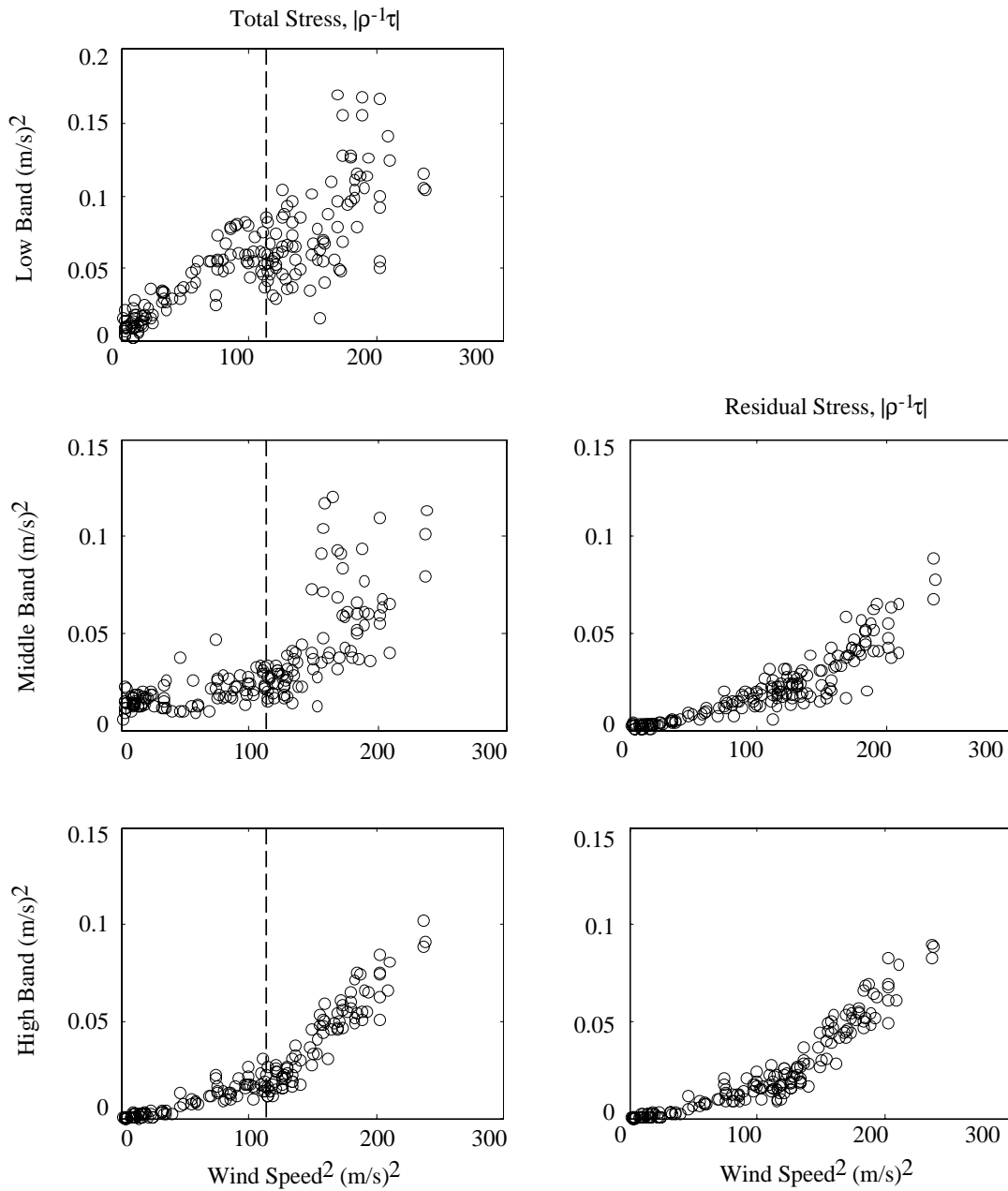


Figure 7. (left) Full and (right) residual wind stress magnitude versus the square of the wind speed, for the (top) low-frequency, (middle) middle-frequency, and (bottom) high-frequency bands. Low-frequency band (top left) varies roughly linearly with wind speed squared, implying a constant drag coefficient best fit. The high-frequency band (bottom left) varies quadratically, implying a wind speed dependent drag coefficient. The middle band (middle left) does not have a clear dependence. As compared with the full stress, the middle band of the residual stress (middle right) exhibits significantly less scatter. In contrast, the high-band residual stress (bottom right) is not appreciably different from the full.

than an order of magnitude smaller than surface elevation at the principal wave frequencies but are dominant at the resonant frequencies of motion (tilt, 0.017 or 58-s period; heave, 0.037 Hz or 27-s period). The motion correction of the surface elevation results in a roughly 70% reduction of energy at the two resonant frequencies, while wave frequencies were modified by $\pm 4\%$ or less. The coherence of heave and tilt displacements with wave elevation are shown in figure 6, bottom. Coherence is very high in the wave band and at the resonant frequencies of FLIP motion.

Because platform motion induced by the waves is itself well correlated with the waves, the contamination due to this motion should affect only the correlated part of the stress, leaving the residual part uncontaminated. The correlated stress estimate (particularly in the middle band) and the total stress (to a lesser extent) are modified by the motion correction, but the residual is not. For the remainder of this paper, “full” stress components refer to the total motion corrected stress data.

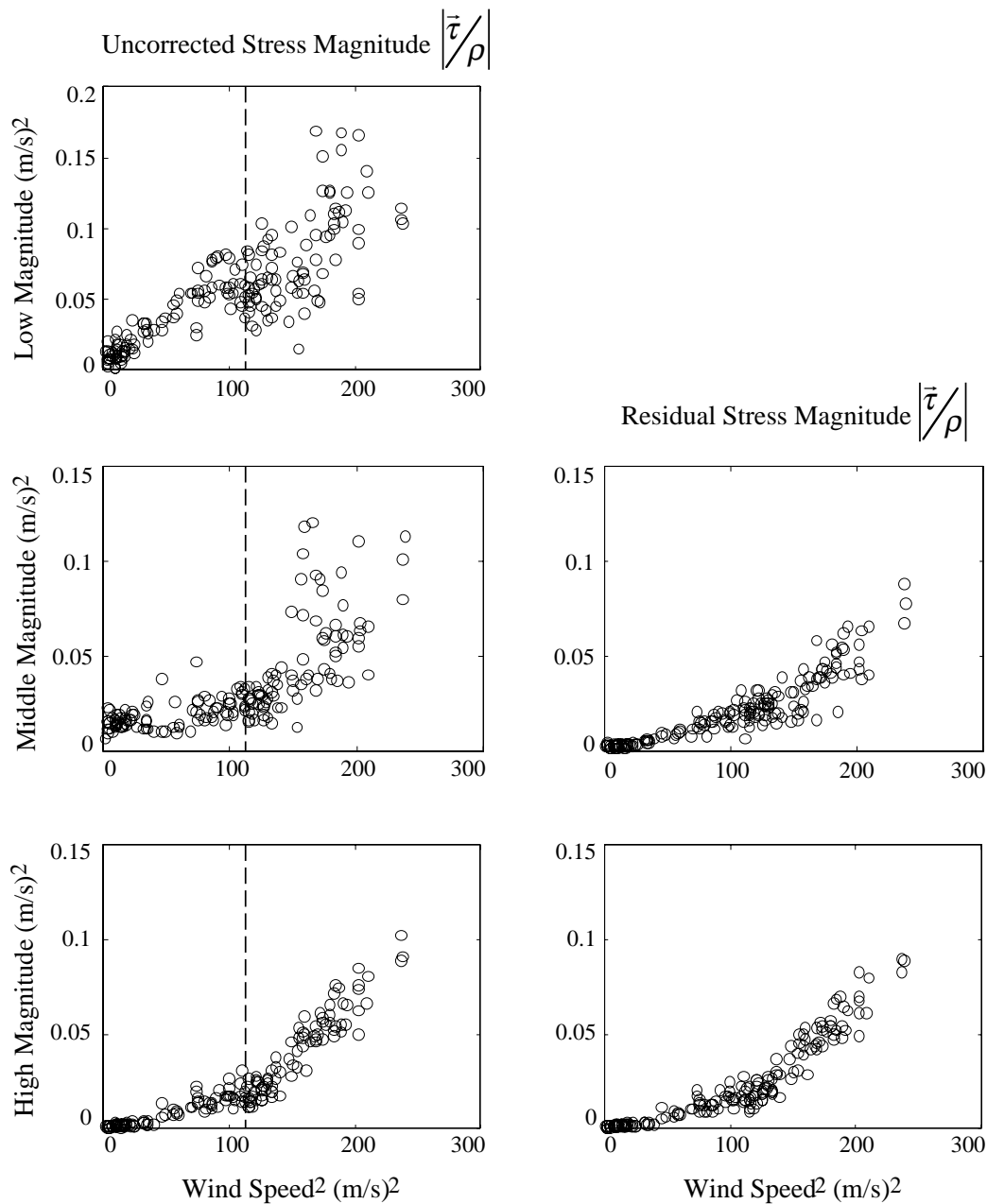


Figure 8. Same as Figure 7, but for data uncorrected for FLIP motion. The magnitudes of the uncorrected stress are slightly different than those for the corrected data, particularly in the middle band. However, the residual stresses are nearly identical, indicating that all motion-induced velocities at the instrument are subsumed in the calculation of the correlated stress.

4. Results

4.1. Magnitude

As implied by (1), the wind stress magnitude is modeled as approximately proportional to the square of the mean wind speed, via an approximately constant drag coefficient. The accuracy of this relation depends on the level of correlation between the stress magnitude and the square of the wind speed. Moreover, the form of correlation (e.g., linear or quadratic) gives a simple indication of how the drag coefficient might depend on wind speed. With this in mind, we plot the magnitudes of the low-, middle-, and high-frequency bands of the full stress (Figure 7, left) and

the middle and high bands of the residual stress (Figure 7, right) against the square of the wind speed. The low-frequency band holds more stress than the other two bands which are of approximately equal size. In all three bands, there seems to be a marked change in the stress magnitude and scatter above approximately 120 (m/s)² or wind speeds greater than 11 m/s. A cutoff around 11 m/s has been previously noted by *Large and Pond* [1981]. In an open ocean data set, they noted that below approximately 11 m/s, the drag coefficient varied little, while above 11 m/s, the drag coefficient showed strong wind speed dependence. Aside from this “global behavior,” we note the following distinguishing features of the behavior in each band.

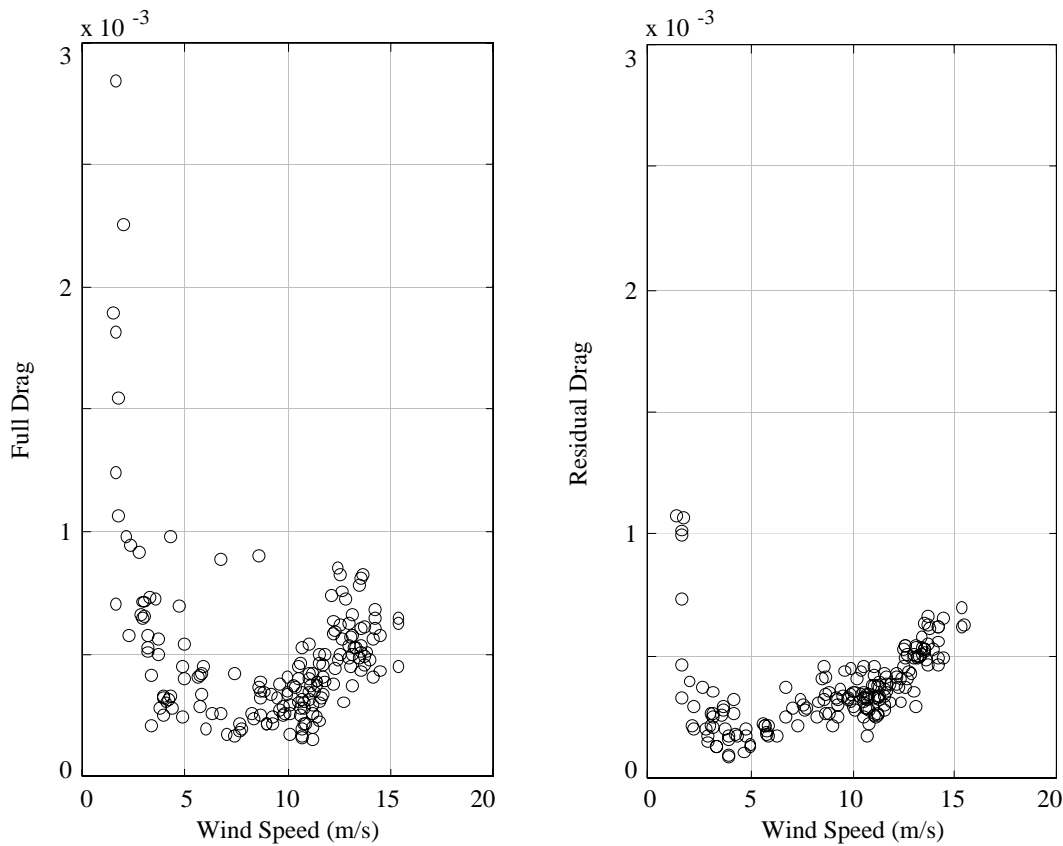


Figure 9. The drag coefficient for the middle plus high band of the full and residual stress versus wind speed for (left) full and (right) residual drag. The full drag shows very large values for low wind speed and large scatter throughout. In contrast, the residual drag is well defined, with less scatter.

The low-frequency band of the full stress (Figure 7, top left) is best fitted by a linear, albeit noisy, regression with wind speed. This indicates that a constant drag coefficient ($C_d = 0.8 \times 10^{-3}$, corresponding to the 8 m height), which explains 67% of the variance in the stress, is the most appropriate.

The high-frequency band (Figure 7, bottom) is best modeled as proportional to wind speed to the fourth power. This fit suggests that the drag coefficient for this portion should be scaled by the square of the wind speed; we interpret this to mean that within this frequency band surface roughness increases dramatically under increased forcing. This form contrasts with the commonly performed linear regression of the (total) drag coefficient against wind speed. The fit for the high-frequency band is good for either the full (Figure 7, bottom left) or residual (Figure 7, bottom right) stress, suggesting that this band is well and simply modeled, and that the waves have little influence other than providing a wind dependent roughness (and affecting the direction; see discussion below).

The middle-frequency band of the full stress (Figure 7, middle left) exhibits a varied wind dependence and does not approach zero for zero wind speed. For low wind speeds, the stress approaches a constant value as wind speed decreases; at higher winds, the stress increases sharply, although not consistently, with increasing wind speed. The failure to approach zero as the wind speed approaches zero explains the large drag coefficients measured at the lowest wind speeds. The middle-frequency residual stress (Figure 7,

right) behaves very differently: it exhibits clear variation with the square of the wind speed, more like the high-frequency band. This stands in stark contrast to the low correlation seen for the full stress. The scatter in full stress is probably attributable to the existence of waves in disequilibrium with the wind. Conceivably, at the lowest wind speeds, incomplete motion correction could contribute to the wave-correlated and hence to the full stress, as well as to its scatter. In any case, having removed the influence of the waves, the residual wind stress is easily modeled.

To demonstrate that FLIP motion effects are also subsumed into the wave correlated stress, we replot Figure 7 using data uncorrected for motion (Figure 8). Some small differences can be seen in the magnitudes of the uncorrected and corrected (full) stresses, particularly in the middle band where the greatest motions occur. In contrast, the magnitude of the residual stress is unchanged. This demonstrates that for an accurate estimate of the residual stress, no motion correction is necessary. This may be a very important fact for stress estimates that are highly contaminated by motion, such as those made from a tilt-and-roll buoy.

We plot drag coefficients corresponding to the full stress (Figure 9, left) and residual stress (Figure 9, right) in the middle and high bands together against wind speed, (all motion corrected). At all wind speeds, the scatter in the drag is significantly reduced after removing the correlated stress: while the full drag shows large scatter, the residual drag shows a clear wind speed dependence. This result indicates a greatly improved ability to model the residual stress fraction

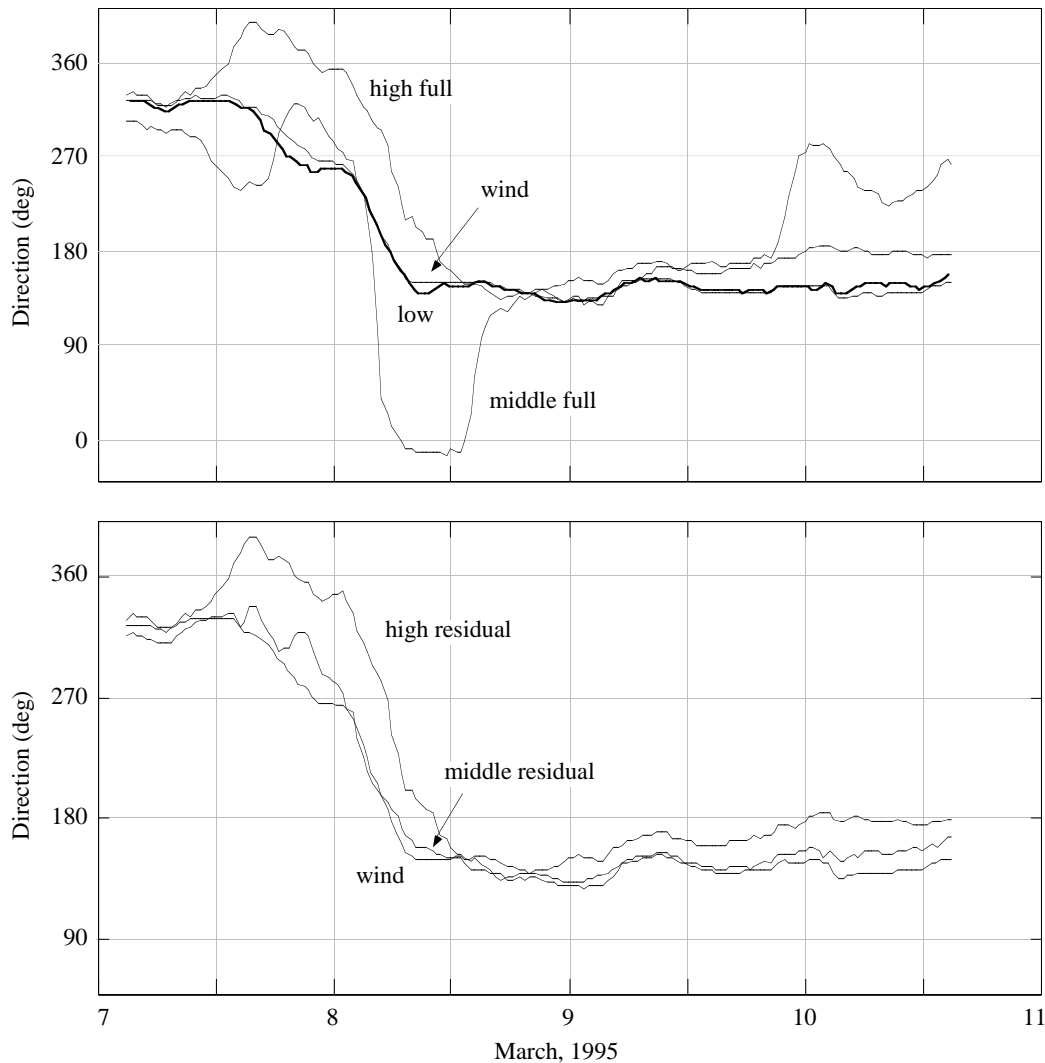


Figure 10. Wind, full stress, and residual stress directions. (top) Direction of the low-frequency band of the full wind stress matches closely that of the wind throughout the period. During the period of turning wind, the high-frequency band lags behind, directed toward the high-frequency sea waves. The middle band is aligned toward the low-frequency swell, particularly during periods of weak winds. (bottom) In contrast, the middle band of the residual stress is well aligned with the wind throughout.

in comparison to the full. For wind speeds greater than 4 m/s, the drag coefficient $C_d = 0.037 \times U - 0.0085 \times 10^{-3}$ has a rms error of 1.16×10^{-4} and explains 83% of the variance in the stress (at all wind speeds). A drag coefficient with second order wind speed dependence, $C_d = .0044 \times U^2 - 0.047 \times U + 0.36 \times 10^{-3}$, has a rms error of 1.05×10^{-4} and explains 87% of the stress variance. At low wind speeds, the residual drag is significantly smaller than the full drag: the correlated stress accounts for a large percentage of the total. At very low wind speeds, the drag coefficient for the residual stress still increases with decreasing wind speed; this could be due to statistical underestimation of the wave-induced fraction. The excellent fit of the residual stress data is a marked improvement over historical at-sea measurements of the wind stress and suggests that the waves are responsible for significant scatter of the drag coefficient.

4.2. Direction

The directions of the various stress components are also important. Previous studies have shown that the wind stress

is often misaligned with the wind, being biased toward the wave direction [Geernaert *et al.*, 1993, Rieder *et al.*, 1994]. This influence is seen here as well. Moreover, the effect is seen only in the middle- and high-frequency bands, where significant wave energy exists, supporting the suggestion that the waves are responsible for the misalignment. Directional differences explain as well why in some cases the residual stress is larger than the full: the correlated and residual stresses oppose each other, so their vector sum is small.

Figure 10 shows time series of the directions of the low-, middle- and high-frequency bands of the full stress (Figure 10, top) and the middle and high bands of the residual wind stress (Figure 10, bottom), smoothed by a 180-min running mean filter. While the direction of the low-frequency stress fraction matches closely that of the mean wind, the middle- and high-frequency bands are often directed away from the wind, toward the waves. During the turning of the wind on March 8, the high-frequency band lags behind and is directed away from the wind toward the high-frequency sea

waves. The middle band, on the other hand, is often greatly misaligned from the wind. The largest misalignments occur during periods when wind speeds decrease, leaving large waves misaligned from the wind and with phase speeds much greater. The residual stress in the middle band, in contrast, is well aligned with the wind throughout the period. Subtracting the correlated portion of the stress from the total effectively removes the influence of the waves on the stress in this band. This further supports the notion that the waves turn the stress. The direction of the high-band residual stress is not well aligned with the wind, just like the high-band full stress. This is probably the result of underestimating the wave-influenced stress for these frequencies: the effect of the waves has not been removed from the wind fluctuations.

The directional misalignment of both high-band stress fractions suggests that the true wave-induced stresses are indeed significant. While motion effects have been removed (directly and by subtraction of the wave-correlated stress), the true wave-induced motions in the air flow are not removed from the stress in this band, leaving residual misalignment that would otherwise be unexplained.

5. Conclusions

By splitting the wind stress into three frequency bands, a low one dominated by large-scale motions in the boundary layer, a middle one influenced by the dominant swell waves, and a high one controlled by the high-frequency equilibrium range waves, the influence of the waves on the wind stress can be partially isolated and examined. The evidence presented here supports the assertion that within the frequency bands where waves exist, the waves have a large effect on the wind stress.

Several effects are noted from the frequency-splitting results. First, the direction of the wind stress is directed away from the mean wind and toward the waves, as suggested by *Geernaert et al.* [1993] and *Rieder et al.*, [1994]. This effect is seen in both the high-frequency seas and lower-frequency swell. In this study, swell redirected the middle band stress away from the wind in one direction, while the high-frequency seas redirected the high band stress in the other. Second, the magnitude of the wind stress is influenced by the waves. The existence of swell in disequilibrium with the local wind adds significant variability to the drag coefficient, as suggested earlier by *Dobson et al.* [1993] and *Rieder* [1997]: in the presence of swell, there is poor correspondence between the middle-band full stress and the wind speed. This contrasts with a strong correspondence for the high-frequency band, which is well modeled by a wind speed dependent drag coefficient. While the high-frequency waves are in near equilibrium with the wind, swell is not. Third, there remain other sources of variability in the wind stress. Significant scatter occurs in the lowest-frequency band, below the frequencies of even the longest waves. This variability could be due to large-scale atmospheric features or could be tied to wave groups and/or breaking. Nonlinear relations such as those suggested by the latter possibility are not investigated here.

Significantly, direct wave influences appear to be effectively quantified by the wave-correlated stress estimate defined in (3). Upon removal of this wave-correlated stress

from the full stress, the troublesome middle-frequency band stress fraction becomes well aligned with the mean wind and is well modeled by a wind speed dependent drag coefficient. The excellent fit of the residual stress data indicates that this approach successfully removes the effect of the waves; conversely, it also indicates that the waves were indeed responsible for the scatter. The correlated stress in the high-frequency band, however, does not eliminate this band's misalignment from the wind. This is suggested to be due to underestimation of the effect on the stress by the corresponding frequency band of waves. These short waves cannot produce significant correlations very far from the surface, so at the height of the anemometer the true influence is underestimated. The height of measurable influence is suggested to be of order k^{-1} .

It should be noted that some of the variability of the stress may be due to an incomplete motion correction of the sonic anemometer data. However, since it has been shown that both the true wave-induced and platform-motion-induced motions are removed with the wave-correlated stress, the results concerning the residual stress stand secure.

6. Discussion

An important goal is to accurately describe the wind stress, under various conditions, from simple measurements of the wind and waves. This study suggests a new approach to this problem. The wind stress can be broken up into three regimes. First, we divide it into a low-frequency part and a high-frequency part, at a frequency just below that of the longest waves under consideration. The low-frequency part is, at present, modeled by a constant drag coefficient and aligned with the mean wind. The direction is accurately modeled, but the magnitude is not. Improvements may be made through further studies of large-scale variability or possibly of wave groupiness or breaking. Second, the high-frequency part is further broken into wave-correlated and residual parts. The residual stress is modeled by a wind speed dependent drag coefficient and is aligned with the mean wind. This study indicates that this portion is then accurately estimated in both direction and magnitude. The remaining portion, the wave-correlated stress, is a logical target for ongoing research.

The wave-correlated stress fraction is the most sensitive of all to platform motion effects, since, in general, it is the waves themselves that cause the motion. We do not investigate the nature of the wave-correlated stress here. The results here strongly suggest that a good model of this wave-induced stress would greatly improve stress estimates in the presence of swell: the fact that the residual stress is well behaved suggests there must be some combination of wind and wave parameters that would work. Furthermore, the wave-induced stress must (nearly) equal the wind input to the waves. This wave growth term is theoretically and empirically well founded only for collinear winds and waves [*Plant*, 1982, *Al-Zanaidi and Hui*, 1984]. Testing of various speculations about the angular dependence of this wave growth term is a logical subject for future study. With the techniques described here, this should be attainable using simple wind and wave information from a suitable variety of conditions.

Acknowledgments. We would like to thank R. Pinkel for the original suggestion to break the stress into frequency bands. We also thank C. Friehe from the University of California, Irvine for loaning us the sonic anemometer used in this study. We also acknowledge the hard work by the members of the Ocean Physics Group at the Scripps Institution of Oceanography: Eric Slater, Lloyd Green, Mike Goldin, and Chris Neely; and by the crew of the research platform *FLIP*, captained by Tom Golfinas. This research was accomplished under grants from the Office of Naval Research N00014-96-1-0030, N00014-93-1-0359, and in part by a grant from Texas A&M University.

References

- Al-Zanaidi, M. A., and W. H. Hui, Turbulent air flow over water waves: a numerical study, *J. Fluid Mech.*, 148, 225-246, 1984.
- Businger, J. A., J. C. Wyngaard, Y. Izumi, and E. F. Bradley, Flux-profile relationships in the atmospheric boundary layer, *J. Atmos. Sci.*, 28, 181-189, 1971.
- Dobson, F. W., S. D. Smith, and R. J. Anderson, Measuring the relationship between wind stress and sea state in the open ocean in the presence of swell, *Atmos.-Ocean*, 32, 237-256, 1993.
- Donelan, M. A., The dependence of the aerodynamic drag coefficient on wave parameters, paper presented at First International Conference on Meteorology and Air/Sea Interaction of the Coastal Zone, Am. Meteorol. Soc., The Hague, Netherlands, 1982.
- Donelan, M. A., F. W. Dobson, S. D. Smith, and R. J. Anderson, On the dependence of sea surface roughness on wave development., *J. Phys. Oceanogr.*, 23, 1993.
- Geernaert, G. L., Measurements of the angle between the wind vector and wind stress vector in the surface layer over the north sea, *J. Geophys. Res.*, 93, 8215-8220, 1988.
- Geernaert, G. L., F. Hansen, M. Courtney, and T. Herbers, Directional attributes of the ocean surface wind stress vector, *J. Geophys. Res.*, 98, 16571-16582, 1993.
- Janssen, P. A. E. M., Wave-induced stress and the drag of air flow over sea wave, *J. Phys. Oceanogr.*, 19, 745-754, 1989.
- Large, W. G., and S. Pond, Open ocean momentum flux measurement in moderate to strong winds, *J. Phys. Oceanogr.*, 11, 324-336, 1981.
- Longuet-Higgins, M. S., D. E. Cartwright, and N. D. Smith, Observations of the directional spectrum of sea waves using the motions of a floating buoy, in *Ocean Wave Spectra: Proceedings of a Conference*, Edited by the National Academy of Sciences, pp. 111-132, Prentice-Hall, Englewood Cliffs, N.J., London, 1963.
- O'Reilly, W. C., T. H. C. Herbers, R. J. Seymour, and R. T. Guza, A comparison of directional buoy and fixed platform measurements of pacific swell, *J. Atmos. Oceanic Technol.*, 13, 231-238, 1996.
- Plant, W. J., A relationship between wind stress and wave slope, *J. Geophys. Res.*, 87, 1961-1967, 1982.
- Rieder, K. F., Analysis of sea surface drag parameterization in open ocean conditions, *Boundary Layer Meteorol.*, 82, 355-377, 1997.
- Rieder, K. F., J. A. Smith, and R. A. Weller, Observed directional characteristics of the wind, wind stress, and surface waves on the open ocean, *J. Geophys. Res.*, 99, 22,589-22,596, 1994.
- Smith, J. A., and K. F. Rieder, Wave induced motion of FLIP, *Ocean Eng.*, 24, 95-110, 1997.

K. F. Rieder and J. A. Smith, Marine Physical Laboratory, Scripps Institution of Oceanography, La Jolla, CA 92093-0213 (e-mail: jasmith@ucsd.edu)

(Received March 24, 1997; revised July 15, 1997; accepted September 8, 1997)